Wordcount results: 6677

Trimethylamine abatement in algal-bacterial photobioreactors

Celia Pascual[1,2], Ilker Akmirza[2,3], Rebeca Pérez[1,2], Esther Arnaiz[1,2], Raúl Muñoz[1,2], Raquel Lebrero[1,2*]

[1]Department of Chemical Engineering and Environmental Technology, University of Valladolid, Dr. Mergelina s/n., Valladolid 47011, Spain

[2]Institute of Sustainable Processes, University of Valladolid, Dr. Mergelina, s/n, 47011, Valladolid, Spain.

[3]Department of Environmental Engineering, Gebze Technical University, Kocaeli, 41400, Turkey

*-Author for correspondence: raquel.lebrero@iq.uva.es

Keywords: Biodegradation, Bubble column bioreactor, Microalgae-bacteria, Odour treatment; Photobioreactor, Trimethylamine.

Abstract

Trimethylamine (TMA) is an odorous volatile organic compound emitted by industries. Algal-based biotechnologies have been proven as a feasible alternative for wastewater treatment, although their application to abate polluted air emissions is still scarce. This work comparatively assessed the removal of TMA in a conventional bacterial bubble column bioreactor (BC) and a novel algal-bacterial bubble column photobioreactor (PBC). The PBC exhibited a superior TMA abatement performance compared to the conventional BC. In this sense, the BC reached a removal efficiency (RE) and an elimination capacity (EC) of 78 % and 12.1 g TMA m^{-3} h^{-1}, respectively, while the PBC achieved a RE of 97 % and a EC of 16.0 g TMA $m^{-3}\cdot h^{-1}$ at an empty bed residence time (EBRT) of 2 min and a TMA concentration ~500 mg m^{-3}. The outstanding performance of the PBC allowed to reduce the operating EBRT to 1.5 and 1 min, while maintaining high REs of 98 and 94 %, and ECs of 21.2 and 28.1 g $m^{-3}\cdot h^{-1}$, respectively. Moreover, the PBC improved the quality of the gas and liquid effluents discharged, showing a net CO_2 consumption and decreasing by ~ 30 % the total nitrogen concentration in the liquid effluent via biomass assimilation. A high specialization of the bacterial community was observed in the PBC, *Mumia* and *Aquamicrobium sp.* being the most abundant genus within the main phyla identified.

1. Introduction

The widespread release of odorous emissions to the atmosphere has become crucial due to their adverse effects on human health and the environment (Xue et al. 2013; Wei et al. 2015). Among odorous compounds, trimethylamine (TMA, C_3H_9N) has been identified as a potentially toxic and likely carcinogenic malodorous volatile organic compound with a low odor threshold concentration of 0.2 µg m^{-3} (Chang et al., 2004). Moreover, TMA exerts a detrimental effect on the synthesis of macromolecules such as DNA, RNA and proteins (Liffourrena and Lucchesi 2014), besides inducing teratogenic effects on animal embryos (Kim et al., 2003). TMA is emitted in wastewater treatment and composting facilities, livestock farms and fish meal manufacturing plants; being partially responsible for the unpleasant odor that characterizes these emissions (Chang et al. 2004; Ding et al. 2008). A proper management of TMA-laden emissions according to environmental regulatory limits is crucial not only to avoid safety and health hazards, but also to mitigate environmental impacts (i.e. greenhouse effect, acid rain and eutrophication) (Chang et al., 2004; Perillo and Rodríguez, 2016).

Biotechnologies have been consistently proven as cost-effective and environmentally friendly alternatives to physical-chemical technologies for the abatement of odorous and toxic gas pollutants (Ho et al. 2008; Estrada et al. 2011). Microorganisms belonging to the genera *Paracoccus, Hyphomicrobium, Pseudomonas, Methylophilus, Arthrobacter, Aminobacter, Haloanaerobacter and Bacillus* are capable of using TMA as the only carbon and energy source (Ding et al. 2008). In addition, previous studies have demonstrated the feasibility of biologically degrading TMA in packed bed bioreactors such as biofilters and biotrickling filters, being the only biotechnology studied up to date (Aguirre et al., 2018; Wan et al., 2011). However, even if high TMA removal rates

have been achieved in these systems, the accumulation of NH_3 (end product of the aerobic oxidation of TMA) typically induces the alkalization of the medium, which ultimately limits TMA biodegradation (Ho et al. 2008). Previous researchers have also evaluated the subsequent NH_3 bio-oxidation to nitrite (NO_2^-) and nitrate (NO_3^-) by heterotrophic bacteria (Oyarzun et al. 2019). However, these nitrogen-containing species remain in the liquid phase resulting in a high nitrogen-loaded effluent.

In the past decades, algal-bacterial based technologies have been widely studied due to their capacity to simultaneously degrading toxic and/or recalcitrant organic materials and depleting nutrients such as ammonium and NO_3^- at high removal rates (Borde et al. 2003; Muñoz and Guieysse 2006). In this context, processes based on the symbiotic interaction between microalgae and bacteria may constitute a competitive alternative to bacterial-based biotechnologies, where TMA is oxidized by bacteria and the N-NH_3 released from TMA oxidation is fixed by microalgae. Microalgae also fix part of the CO_2 produced in the bacterial oxidation of TMA and provide oxygen during the photosynthetic activity, thus reducing the CO_2 footprint and the aeration needs of the process (Kang et al. 2017). Moreover, the biomass generated in these processes can be further valorized as biofuel feedstock or as biofertilizer (Muñoz and Guieysse, 2006). Despite the above mentioned advantages, the implementation of algal-bacterial processes for waste gas treatment has been scarcely studied. In this regard, the configuration of the photobioreactor is of key relevance since it determines the efficiency of light penetration in the algal-bacterial cultivation broth. Bubble column reactors guarantee construction and operation simplicity (Chang et al. 2017; Merchuket al. 2007), provide a high mass and heat transfer efficiency, and present low operating costs (Vo et al. 2018; Zhang et al. 2018).

This research comparatively investigated the TMA removal performance of a bacterial bubble column bioreactor (BC) and an algal-bacterial bubble column photobioreactor (PBC), with a special focus on the quality of the treated gas (TMA and CO_2 concentrations) and liquid effluent (concentration of N-containing species). The structure of the microbial community in the PBC was also analyzed by pyrosequencing.

2 Materials and Methods

2.1 Inoculum

Activated sludge from Valladolid wastewater treatment plant (Valladolid, Spain) was used to inoculate the BC, while a mixed inoculum containing activated sludge and microalgae (1:1 v/v) was employed for the inoculation of the PBC. The microalgae were obtained from a biogas upgrading high rate algal pond located at the Department of Chemical Engineering and Environmental Technology at the University of Valladolid (Valladolid, Spain) and operating with a total suspended solids (TSS) concentration of 1.62 g L^{-1} and a volatile suspended solids concentration (VSS) of 1.48 g L^{-1} (Franco-Morgado et al. 2017).

2.2 Chemicals and mineral salt medium

The mineral salt medium (MSM) was composed of (g L^{-1}): $Na_2HPO_4 \cdot 12H_2O$, 6.15; KH_2PO_4, 1.52; $MgSO_4 \cdot 7H_2O$, 0.2; $CaCl_2$, 0.038; and 10 mL L^{-1} of a SL4 solution containing (g L^{-1}): EDTA, 0.5; $FeSO_4 \cdot 7H_2O$, 0.2; $ZnSO_4 \cdot 7H_2O$, 0.01; $MnCl_2 \cdot 7H_2O$, 0.003. All the chemicals used for the preparation of the MSM were purchased in Panreac (Barcelona, Spain). Trimethylamine (45 % purity) was obtained from Sigma Aldrich (San Luis, EEUU).

2.3 Experimental setup and operating procedure

The experimental setup (Fig. 1) consisted of two cylindrical PVC columns (height = 0.58 m; inner diameter = 0.094 m) with a working volume of 4 L. The synthetic contaminated emission was prepared by injecting the TMA liquid solution with a syringe pump (Fusion 100, Chemyx Inc. USA) into an air stream of 2 L min^{-1}, resulting in an average inlet concentration of 513 ± 69 mg m^{-3} in each bioreactor. The gas stream entered a mixing chamber in order to ensure complete TMA evaporation and homogenization before being fed to the reactors through a porous diffuser (pore diameter of 10 μm) located at the bottom.

For the inoculation of the BC, 2 L of aerobic activated sludge were centrifuged for 10 min at 10000 rpm and the pellet was resuspended in 1 L of MSM. The inoculum was added to the BC and fresh MSM was supplemented upon filling the 4 L of working volume, resulting in TSS and VSS concentrations of 2.79 and 2.13 g L^{-1}, respectively. The BC was operated for 78 days at an empty bed residence time (EBRT) of 2 min and a daily replacement of 250 mL of the culture broth with fresh MSM (equivalent to a dilution rate of 0.0625 d^{-1}). During the first 50 days of operation, all the biomass was recovered from the retrieved cultivation broth by centrifugation and returned to the bioreactor (equivalent to an infinite solids retention time) in order to promote biomass accumulation until reaching ~ 3 g VSS L^{-1}. From day 50 onwards, 75 mL of the 250 mL of the cultivation broth daily retrieved were discarded (cell retention time = 53.3 days) in order to maintain a constant VSS concentration in the bioreactor.

A 1 h abiotic test was performed with no biomass prior PCB start-up. For this purpose, the PCB illuminated with the LED lights was filled with mineral medium and TMA was continuously supplied at an inlet concentration of ~700 mg m^{-3}. The results demonstrated that no TMA was removed by either adsorption or photodegradation

(Supplementary materials, Fig. S1). The inoculation of the PBC was performed by centrifugation of 1 L of aerobic activated sludge and 1 L of microalgae culture (10 min, 10000 rpm). The pellets were resuspended in 1 L of MSM, added to the PBC and filled up to 4 L with fresh MSM at initial TSS and VSS concentrations of 2.18 and 1.76 g L^{-1}, respectively. The PBC was operated for 103 days. CO_2 was added to the inlet TMA-laden emission at a concentration of 6 % v/v in order to supply inorganic carbon for photosynthetic microalgae growth. To this end, 1.88 L min^{-1} of TMA-laden air were mixed with 0.12 L min^{-1} of pure CO_2 (Abelló Linde, Spain). A set of LED was installed around the PBC, providing a photosynthetic active radiation (PAR) of ~ 250 µmol m^{-2} s^{-1} at the outer reactor surface. The PBC was operated during the first 54 days at an EBRT of 2 min with a daily MSM exchange rate of 250 mL (equivalent to a dilution rate of 0.0625 d^{-1}) (Stage I). Between days 55 and 79, the EBRT was reduced to 1.5 min and the MSM exchange rate increased up to 375 mL d^{-1} (Stage II). Finally, from day 80 onwards, the EBRT was further decreased to 1 min and 500 mL of MSM were daily exchanged (Stage III). During the first 12 days of operation, the biomass was recovered from the withdrawn cultivation broth and returned to the PBC after centrifugation in order to increase VSS concentration in the reactor. From this day on, the amount of biomass returned to the system was adjusted in order to maintain a constant biomass concentration of 3.5 g VSS L^{-1}.

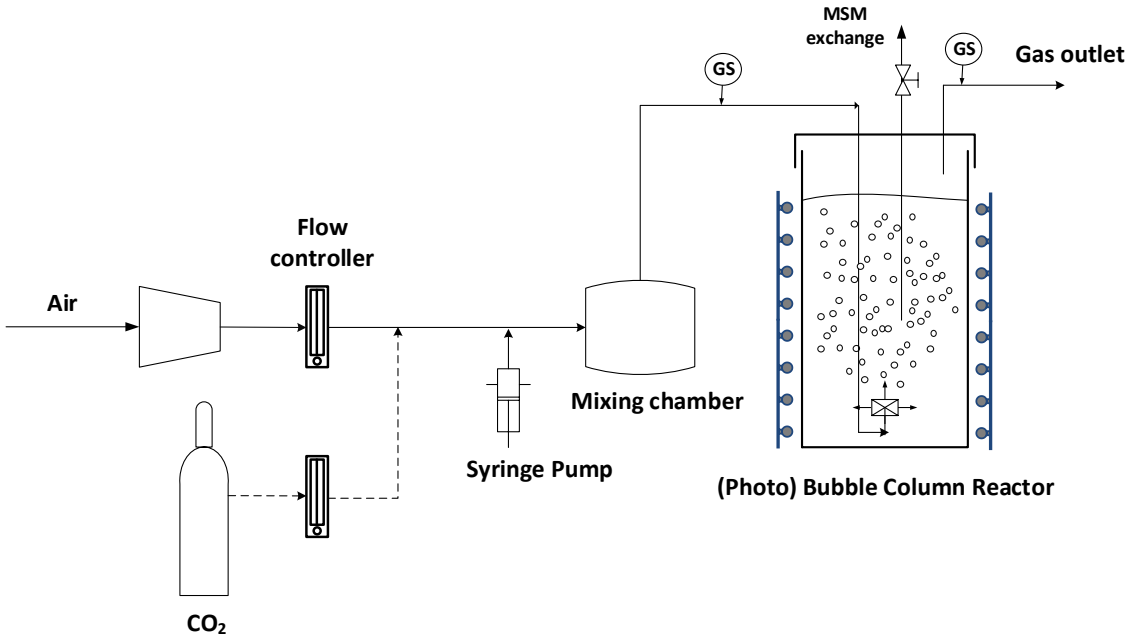

Fig. 1 Schematic representation of the experimental setup. GS: Gas sampling port

2.4 Analytical procedure

TMA gas concentration was analyzed in a Bruker 3900 gas chromatograph (Palo Alto, USA) equipped with a flame ionization detector and a Supelco HP-5-MS (30 m × 0.25 µm × 0.25 µm) column. The oven, detector and injector temperatures were maintained constant at 250, 300 and 200 °C, respectively, for 2.5 min. N_2 was used as the carrier gas at a flow of 1 mL min^{-1}. CO_2 and O_2 gas concentrations were determined in a Bruker 430 gas chromatograph (Palo Alto, USA) coupled with a thermal conductivity detector and equipped with a CP-Molsieve 5A (15 m × 0.53 µm × 15 µm) and a P-PoraBOND Q (25 m × 0.53 µm × 10 µm) columns. Oven, detector and injector temperatures were maintained constant at 45, 200 and 150 °C for 5 min, respectively. Helium was used as the carrier gas at a flow of 13.7 mL min^{-1}. The pressure in the inlet gas stream was daily measured using a differential pressure sensor IFM (Essen, Germany) in order to control the actual flow of the inlet gas into the reactor.

The pH was daily analyzed in the cultivation broth using a glass membrane electrode PH BASIC 20 (Crison, Barcelona, Spain). Dissolved oxygen (DO) and temperature were also analyzed in the cultivation broth of the PBC using a CellOx 325 oxygen meter with a temperature sensor (WTW, New York, EEUU). Samples of the liquid phase of both bioreactors were drawn twice a week for the determination of TSS, total organic carbon (TOC), inorganic carbon (IC), total nitrogen (TN), ammonia (NH_4^+), NO_2^- and NO_3^- concentrations. TSS and VSS concentrations were determined according to standard methods (American Water Works Association, 2012). TOC, IC and TN concentrations were measured using a TOC-VCSH analyzer coupled with a TNM-1 chemiluminescence module (Shimadzu, Japan). NH_4^+ concentration was analyzed with an Orion Dual Star ammonium specific electrode (Thermo Scientific, The Netherlands). Finally, 1 mL samples of cultivation broth were filtered through 0.22 μm filters and analyzed by HPLC-IC for nitrite and nitrate determination using a Waters 515 HPLC pump coupled with a conductivity detector (Waters 432) and equipped with an IC-PAK Anion HC column (4.6 × 150 mm) and an IC-Pak Anion Guard-Pak (Waters). Samples were eluted isocratically at 2 mL min^{-1} (at room temperature) with a solution of distilled water/acetonitrile/n-butanol/buffer at 84/12/2/2% v/v (Muñoz et al. 2013). The determination of the elemental composition of the algal-bacterial biomass in terms of carbon (C), hydrogen (H) and nitrogen (N) content was conducted at the end of the experimental period using a LECO CHNS-932 analyzer.

2.5 DNA extraction, illumina library preparation and pyrosequencing

Two samples were drawn for biological analysis from the cultivation broth of the PBC: I-PBC (corresponding to the algal-bacterial inoculum) and F-PBC (at the end of the experimental period). Total genomic DNA was extracted from 500 μL of sample using

the Fast DNA Spin kit for soil (Biomedical, USA) according to the manufacturer's instructions. DNA concentration was estimated by the Qubit fluorometer from Invitrogen, and the final concentration of the DNA sample was normalized to 5 ng μL^{-1}. The extracted DNA was stored at -20ºC prior to pyrosequencing. Amplicon sequencing was carried out targeting the 16S V3 and V4 regions (464bp, *Escherichia coli* based coordinates) with the bacterial primers S-D-Bact-0341-b-S-17 and S-D-Bact-0785-a- A-21, forward and reverse, respectively, which were chosen according to (Klindworth et al. 2013). Illumina adapter overhang nucleotide sequences were added to the gene-specific sequences, thus resulting in the following full-length primers for the analysis: 5´TCGTCGGCAGCGTCAGATGTGTATAAGAGACAGCCTACGGGNGGCWGCAG (16S amplicon PCR forward primer), and 5´GTCTCGTGGGCTCGGAGATGTGTATAAGAGAC-AGGACTACHVGGGTATCTAATCC (16S amplicon PCR reverse primer). Indexed paired-end libraries were generated using the Nextera XT DNA Sample Preparation Kit (Illumina, San Diego, CA), with a reduced number of PCR cycles (25) using 55 ºC as annealing temperature. Libraries were then normalized and pooled prior to sequencing. Non-indexed PhiX library (Illumina, San Diego, CA) was used as performance control. Samples containing indexed amplicons were loaded onto the MiSeq reagent cartridge and onto the instrument along with the flow cell for automated cluster generation and paired-end sequencing with dual s (2 × 300bp run, MiSeq Reagent Kit v3) (Illumina, San Diego, CA). The pyrosequencing analysis was carried by the Foundation for the Promotion of Health and Biomedical Research of Valencia Region (FISABIO, Spain).

2.6 16S rDNA-based taxonomic analysis

Quality assessment was performed using the PRINSEQ-LITE program (Schmieder and Edwards 2011) applying the following parameters: min_length: 50, trim_qual_right: 30, trim_qual_type: mean and trim_qual_window: 20. After quality assessment, paired-end reads were joined together with the FLASH program (Magoč and Salzberg 2011). The eventual chimeras belonging to PCR artifacts among the sequences were discarded using the USEARCH program (Edgar 2010), and taxonomic assignments were then carried out using the RDP- Classifier from the Ribosomal Database Project (Wang et al. 2007; Cole et al. 2009), which is available from the RDP website (http://rdp.cme.msu.edu/ classifier/). Shannon index was calculated using the Vegan library version 2.3e1 (Oksanen et al. 2015). The Krona tool was used to represent relative abundances and confidences within the complex hierarchies of metagenomics classifications (Ondov et al. 2011).

2.7 Data analysis

The statistical data analysis was performed using SPSS 20.0 (IBM, USA). The results are given as the average ± standard deviation. Significant differences were analyzed by ANOVA and post-hoc analysis for multiple group comparisons. Differences were considered to be significant at $p \leq 0.05$.

3. Results and discussion

3.1 Performance of the bacterial bioreactor

TMA removal efficiency (RE) reached values of ~ 80 % immediately after BC start-up, recording an average removal of 78 ± 5 % during the complete experimental period

(Fig. 2A, white bars). The maximum RE (88.3 %) was observed by day 52 of operation, corresponding to an inlet TMA concentration of 658 mg m^{-3}. The average elimination capacity (EC) of the system was 12.1 ± 2.2 g TMA m^{-3} h^{-1}, and the maximum EC value of 16.7 g TMA m^{-3} h^{-1} was achieved by day 64 at an inlet TMA concentration of 638 mg m^{-3}.

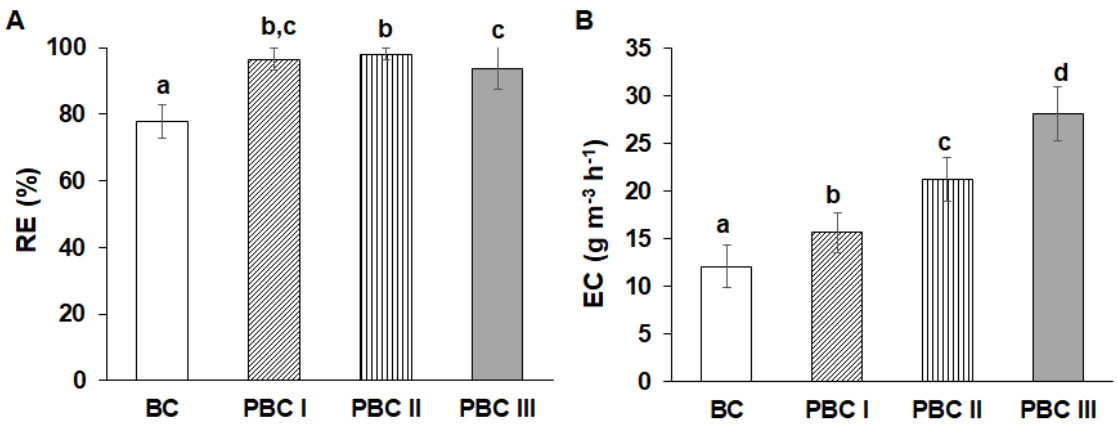

Fig. 2 Average TMA removal efficiencies (A) and elimination capacities (B) in the BC (white bars) and the PBC at the three EBRTs tested: (I) 2 min, (II) 1.5 min and (III) 1 min. Vertical lines represent standard deviation from replicate measurement under steady state. Columns within each group with different letters were significantly different at $p < 0.05$

A high CO_2 production was recorded right after the start-up of the BC, reaching a maximum concentration of 5.8 g m^{-3} by day 3 of operation. This high production rate (121.9 g CO_2 m^{-3} h^{-1}) was attributed to the degradation of both TMA and cell debris and death biomass from the inoculum. From this day on, CO_2 concentration gradually decreased until stabilizing at 1.6 ± 0.7 g m^{-3} from day 27 onwards. The activation of nitrifying bacteria, autotrophic consumers of CO_2, likely contributed to the reduction of the emitted CO_2, with final production values of 27.9 g CO_2 m^{-3} h^{-1}.

Ammonia was produced during the aerobic degradation of TMA, and its accumulation in the cultivation broth might result in inhibitory effects on the microbial community. Thus, the analysis of the variation of the pH and the nitrogen species concentration in the liquid phase is of key importance in biological reactors devoted to TMA removal. From day 0 to 10, the pH fluctuated between 7 and 8, this neutral value being likely associated with NH_4^+ accumulation (NH_4^+ concentration in the cultivation broth increased up to 365 mg N-NH_4^+ L^{-1} by day 10). This behavior has been previously reported in biofilters treating TMA (Ho et al. 2008). During these days, neither NO_2^- nor NO_3^- accumulation was observed (Fig. 3A). Between days 11 and 50, a gradual decrease in the pH was recorded, reaching a minimum value of 4.21 on day 49 (Fig. S2A). This pH decrease was attributed to the activation of nitrifying bacteria, which mediated the oxidation of NH_4^+ to NO_3^- up to a maximum value of 830 mg N-NO_3^- L^{-1} by day 45 and triggered the acidification of the cultivation broth. Similarly, Ho et al. (2008) observed an increase in nitrite and nitrate concentration and a decrease in NH_4^+ concentration when species of nitrifying bacteria were inoculated in their biotrickling filter. In our particular case, NO_2^- accumulation was negligible compared to NO_3^- accumulation. The concentration of nitrogen species in the culture medium finally stabilized at steady state values of 411 ± 79 mg N-NH_4^+ L^{-1} and 793 ± 96 mg N- NO_3^- L^{-1} (average pH of 5.4 ± 0.4). Despite the high concentrations of NH_4^+ and NO_3^-, no toxic effect was observed on the microbial community, which was able to maintain constant TMA degradation regardless of the pH of the culture broth.

An initial decrease in the VSS concentration was observed due to cell lysis, reaching a minimum value of 1.07 g L^{-1} by day 4 (Fig. S3A). From day 4 onwards, the VSS concentration gradually increased up to a maximum value of 3.74 g L^{-1} by day 45.

Finally, a steady concentration of 3.0 ± 0.1 g L^{-1} was maintained by setting a constant solids retention time.

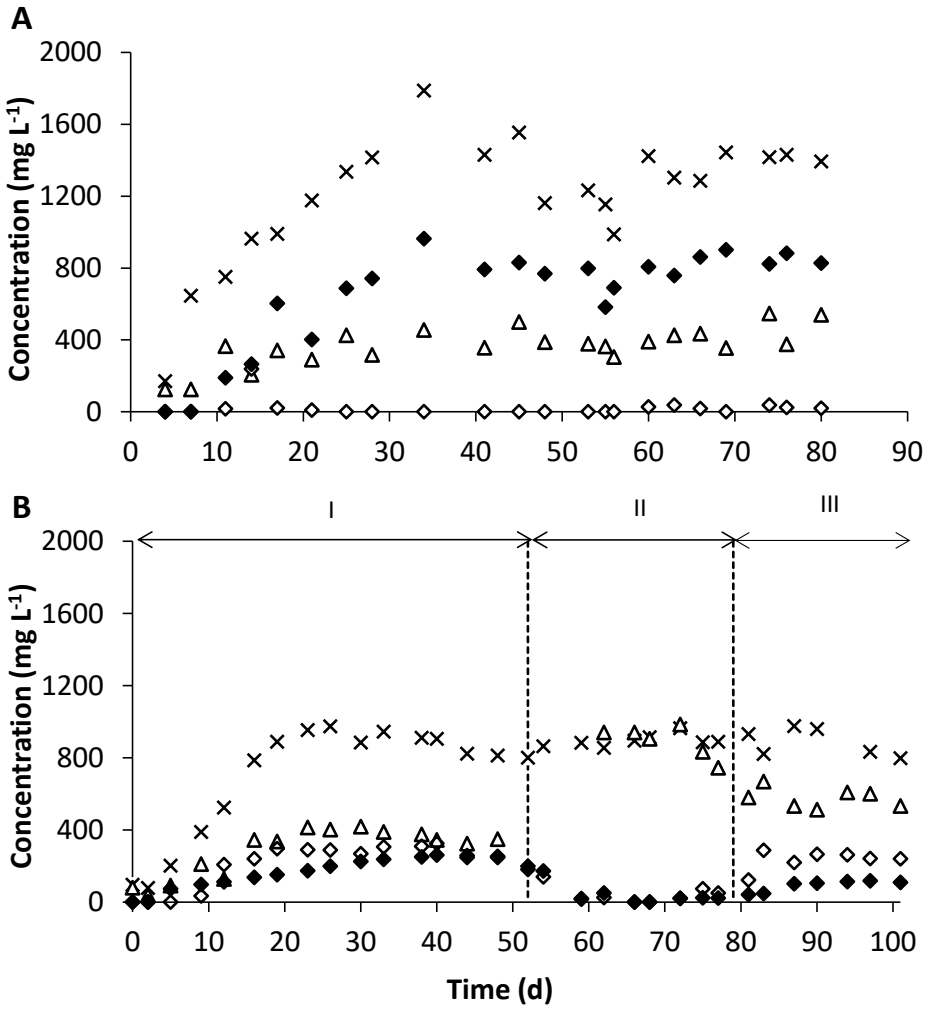

Fig. 3 Time course of the nitrogen species in BC (A) and PBC (B): TN (×), N-NH_4^+ (Δ), N-NO_3^- (♦) and N-NO_2^- (◊)

3.2 Performance of the algal-bacterial photobioreactor

A high TMA removal performance was recorded following PBC start-up. REs and ECs remained at average values of 97 ± 3 % and 16.0 ± 2.1 g m^{-3} h^{-1}, respectively, during process operation at an EBRT of 2 min (Fig. 2). TMA outlet concentrations were significantly lower compared to those recorded in the BC, with average values of 22 ±

18 mg m^{-3}. The outlet TMA concentration was even below the detection limit of the GC-FID (~3.6 mg m^{-3}) on certain days of operation. A maximum EC of 18.5 g m^{-3} h^{-1} was recorded on day 4, corresponding to a TMA inlet concentration of 655 mg m^{-3}. The good performance of the photobioreactor allowed to further reducing the EBRT to 1.5 min (stage II) and 1 min (stage III). This decrease in EBRT did not mediate a deterioration in process performance as shown by the high REs of 98 ± 2 % and 94 ± 6 % recorded in stage II and III, respectively. The increase in TMA load resulted in significantly higher ECs under these operating conditions (21.2 ± 2.3 and 28.1 ± 2.8 g $m^{-3}\cdot h^{-1}$, respectively) (Fig. 2B). These results were considerably better than those obtained in previous TMA biodegradation studies reported in literature. For instance, Wan et al. (2011) recorded a RE of ~79 % (maximum EC of 14.0 g TMA m^{-3} h^{-1}) in a biotrickling filter treating a contaminated emission polluted with 420 mg m^{-3} of TMA at an EBRT of 1 min.

A net CO_2 consumption of ~9 % (taking into account the CO_2 supplemented and CO_2 produced by heterotrophic bacteria) was recorded throughout the experimental period as a result of inorganic carbon assimilation by microalgae and nitrifying bacteria. An average CO_2 concentration value of 151.8 ± 21.0 g m^{-3} was obtained regardless of the operating conditions. On the other hand, the outlet O_2 concentration always exceeded the inlet concentration value.

NH_4^+ concentration steadily increased after PBC start-up at an EBRT of 2 min, reaching a steady value of 369 ± 34 mg N-NH_4^+ L^{-1} from day 16 onwards. However, nitrifying activity was recorded earlier in the PBC compared to the BC, resulting in the accumulation of NO_3^- and NO_2^- from days 5 and 9, respectively. In addition, NO_2^- concentration increased above NO_3^- concentration by day 12. From day 33 onwards, these nitrogen species stabilized at 290 ± 33 mg N-NO_2^- L^{-1} and 248 ± 8 mg N-NO_3^- L^{-1}

(Fig. 3B). When the EBRT was reduced to 1.5 min (stage II), the increase in TMA load resulted in a sharp decrease in the concentration of both nitrite and nitrate to steady values of 48 ± 27 mg N-NO_2^- L^{-1} and 22 ± 2 mg N-NO_3^- L^{-1} during this stage. On the contrary, ammonia concentration increased up to 853 ± 121 mg N-NH_4^+ L^{-1}, which suggested a inhibition of the nitrifying bacteria as a result of their high sensitivity to ammonia loading (Awolusi et al. 2016). A slight recovery of the nitrifying activity was observed during stage III, where ammonia concentration decreased to 593 ± 60 mg N-NH_4^+ L^{-1} and nitrate and nitrite concentrations increased to steady values of 111 ± 6 mg N-NO_3^- L^{-1} and 252 ± 23 mg N-NO_2^- L^{-1}, respectively (Fig. 3B).

An average temperature of 30.7 ± 1.0 ºC was recorded in the PBC cultivation broth, slightly higher than the temperature recorded in BC (25 ºC) due to the illumination of the reactor with LED lights. The DO in the medium remained at 5.7 ± 0.8, 6.7 ± 0.4 and 7.2 ± 0.2 mg L^{-1} in stages I, II and III, respectively, always below water saturation at the operating temperature (7.6 mg L^{-1}) due to the active aerobic degradation of TMA. The increase in the DO when decreasing the EBRT can be attributed to the higher mass transfer coefficient (K_La) resulting from the higher gas flowrates, and thereby an enhanced O_2 transfer to the liquid medium. Values of DO and O_2 concentration in the treated gas stream confirmed that the system was not limited by oxygen availability. The pH remained roughly constant throughout the complete experimental period, with average values of 6.7 ± 0.3, 7.7 ± 0.2 and 7.4 ± 0.2 at stages I, II and III, respectively (Fig. S2B).

A decrease in VSS concentration was observed during the first operating days, reaching a minimum value of 1.15 g L^{-1}. From day 5, biomass concentration increased up to 3.84 g VSS L^{-1} by day 12 (Fig. S3B). A daily biomass wastage was then implemented in order to maintain constant VSS concentrations of 3.13 ± 1.04, 4.41 ± 0.39 and 3.65 ±

0.61 g L^{-1}, in stages I, II and III, respectively. It is important to remark that a higher biomass growth was recorded in the PBC compared to the BC due to the contribution of the algal biomass.

3.3 Comparative analysis between BC and PBC

Overall, the PBC showed a better TMA removal performance than the conventional BC at an EBRT of 2 min, with EC ×1.3 times higher compared to those recorded in the BC at this EBRT. This improved behavior was attributed to the higher pH prevailing in the PBC, which remained close to optimum values (6-8) for the enzymatic activity of TMA-degrading bacteria (Chang et al. 2004). In this context, the pH in BC remained below this optimal interval likely due to nitrification, while an average value of 6.7 ± 0.3 was recorded in the PCB due to N assimilation by microalgae and the inherent increase in pH caused by photosynthesis. These favorable environmental conditions allowed reducing the EBRT in the PCB to 1 min without statistically significant differences in the RE and higher ECs (up to ×2.3 higher), despite the increase in TMA load. This fact was attributed to a mass transfer limitation rather than a biological limitation in the photobioreactor. In this sense, an increase in the TMA load resulted in a higher concentration gradient and therefore an enhanced TMA mass transfer from the gas to the liquid phase, where TMA-degrading microorganisms were capable of sustaining the removal performance of the system.

Likewise, an improvement in the quality of the liquid effluent in terms of N content under comparable TMA removal efficiencies was observed in the PBC. A total nitrogen mass balance showed that 30% less nitrogen was discharged in the exchanged PBC cultivation broth compared to that of the BC, even at EBRTs of 1.5 and 1 min (when TMA load was 1.5 and 2 times higher, respectively) (Fig. 4). TN concentration

decreased significantly from 1307 ± 149 mg N L^{-1} in the BC to 879 ± 58, 893 ± 39 and 886 ± 78 mg N L^{-1} in the PBC in stages I, II and III, respectively. This decrease was associated to nitrogen assimilation during algal biomass growth. Indeed, a biomass production of ~0.23 and 0.70 g biomass d^{-1} was recorded in the BC and the PBC, respectively. In this context, nitrogen is the most abundant macronutrient in algal biomass with a content ranging between 5 and 10 % of its dry weight, as confirmed by the analysis of CHN content of algal-bacterial biomass (42.3 ± 4.2 % C, 6.0 ± 0.6 % H and 6.2 ± 1.3 % N). Nitrogen can be assimilated in the forms of NO_3^-, NO_2^-, NO or NH_4^+, although assimilation of NH_4^+ over nitrite and nitrate is preferred by microalgae as a result of its most reduced redox state (Markou et al. 2014). Interestingly, NO_2^- concentration increased in the PBC during stage I while an increase in NH_4^+ concentration was recorded during stage II. This was attributed to the different activity of the bacteria involved in the nitrification process depending on the operating conditions of the PBC, resulting in the inhibition of the different stages of nitrification, where ammonia oxidizing bacteria (AOB) oxidize NH_4^+ to NO_2^-, which is subsequently oxidized to NO_3^- by nitrite-oxidizing bacteria (NOB). In this regard, the accumulation of nitrite in stage I was attributed to the partial nitrification of NH_4^+ as a result of the high temperature in the reactor (~31 ºC), which could hinder the activity of NOB such as *Nitrobacter* (optimum temperature range ~ 24–25 °C) (Huang et al. 2010; Awolusi et al. 2016). Thus, an incomplete nitrification would trigger the accumulation of NO_2^- in the medium. On the other hand, NH_4^+ concentration increased in stage II. The higher TMA load applied at this lower EBRT might have inhibited nitrifying bacteria activity due to their greater sensitivity to changes in NH_4^+ loading rates (Hu et al. 2009; Awolusi et al. 2016), thus preventing NH_4^+ nitrification. In stage III, NO_2^- concentration

significantly increased up to values close to those of stage I, probably due to the acclimation of nitrifying bacteria to the temperature and NH_4^+ loading rates.

Overall, the optimal operating conditions were recorded in the PBC during Stage III since similar values of TMA RE (> 90 %) and total nitrogen concentration in the exchanged cultivation broth were recorded compared to Stages I and II, while the TMA elimination capacity increased by ×2.3.

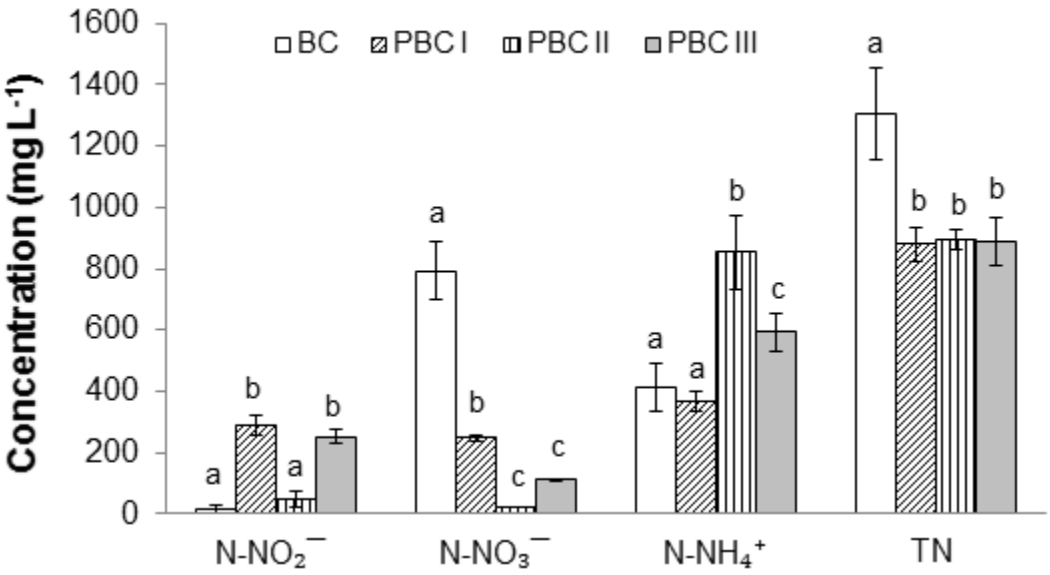

Fig. 4 Concentration profiles of nitrogen-containing species in the BC (white columns) and PBC at the three EBRTs tested: (I) 2 min, (II) 1.5 min and (III) 1 min. Vertical lines represent standard deviation. Columns within each group with different letters were significantly different at $p < 0.05$

3.4 Effect of trimethylamine on the microbial communities

A total of 133521 and 105547 initial bacterial 16S rRNA sequence reads generated by the MiSeq Illumina platform for I-PBC and F-PBC samples, respectively, passed the quality and taxonomic cutoff. Effective bacterial sequences from the samples were

affiliated to a total of 11 phyla. Of them, the most dominant phyla in I-PBC were *Actinobacteria* (32 %), *Proteobacteria* (17 %), *Candidatus Saccharibacteria* (15 %), *Chloroflexi* (11 %) and *Firmicutes* (9 %). Other phyla with abundances > 1 % were *Bacteroidetes*, *Planctomycetes* and *Verrucomicrobia*. These phyla are commonly found in activated sludge (Zhang et al. 2012; Lebrero et al. 2013). However, a significant specialization of the microbial community was observed as a result of TMA biodegradation, which resulted in the dominance of only two phyla: *Actinobacteria* (55 %) and *Proteobacteria* (42 %) (Fig. 5). Indeed, the Shannon-Wiener diversity indices of the microbial communities present at the I-PBC and F-PBC were 3.68 and 1.86, respectively. Typical values range from 1.5 to 3.5, which correspond to low and high species evenness and richness, respectively (MacDonald 2003). The significant decrease in the diversity index revealed a gradual enrichment and specialization of the microbial community as a result of TMA biodegradation.

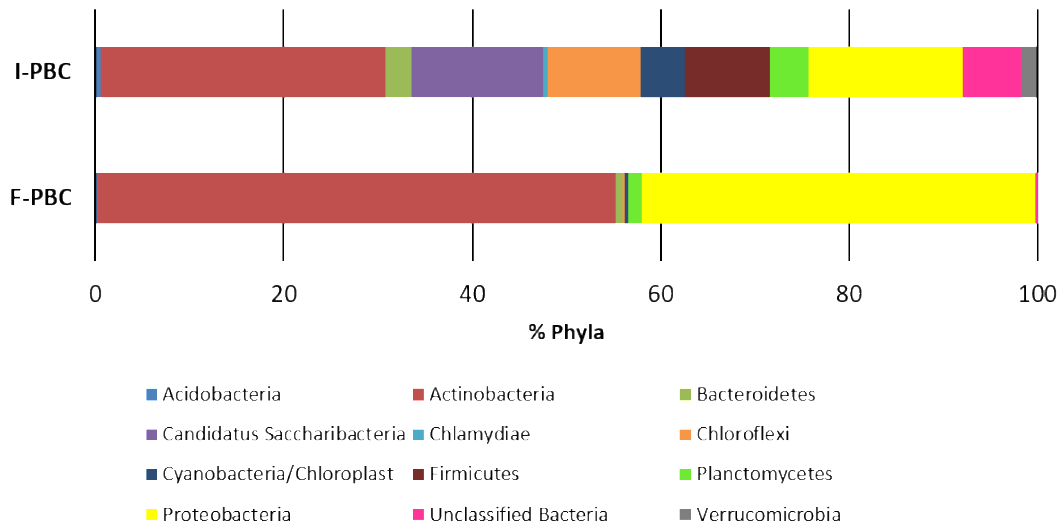

Fig. 5 Community composition at a phyla level across samples. I-PBC: algal-bacterial inoculum, F-PBC: end of the experimental period. The abundance is presented in terms of percentage in total effective bacterial sequences in a sample, classified using RDP Classifier

At the genus level, the pyrosequencing showed a total of 501 genera in I-PBC and 139 in F-PBC sample (Fig. 6). Of them, only 82 in I-PBC and 20 in F-PBC were present with abundances > 0.1 % (Table S1), and represented 95 and 98 % of the total number of readings at the genus level, respectively, which confirmed the lower diversity in the F-PBC. Based on the phylogenetic analysis, the *Actinobacteria* phylum was the most abundant in both samples, the genus *Mumia*, belonging to the family *Nocardioidaceae*, representing 47 % of the total genera. The *Mumia* genus was recently discovered in soil samples (Lee et al. 2014), thus growth conditions and functions are yet unknown. The results obtained in the present study suggest the ability of *Mumia* to grow on TMA, although further research is necessary to confirm this hypothesis.

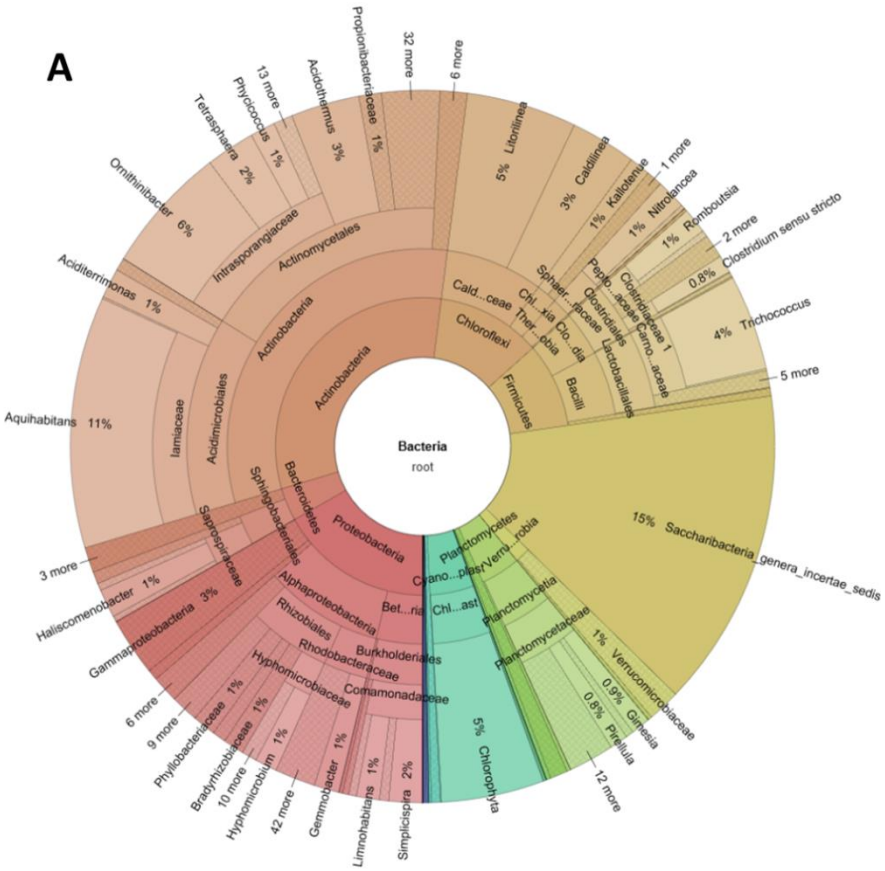

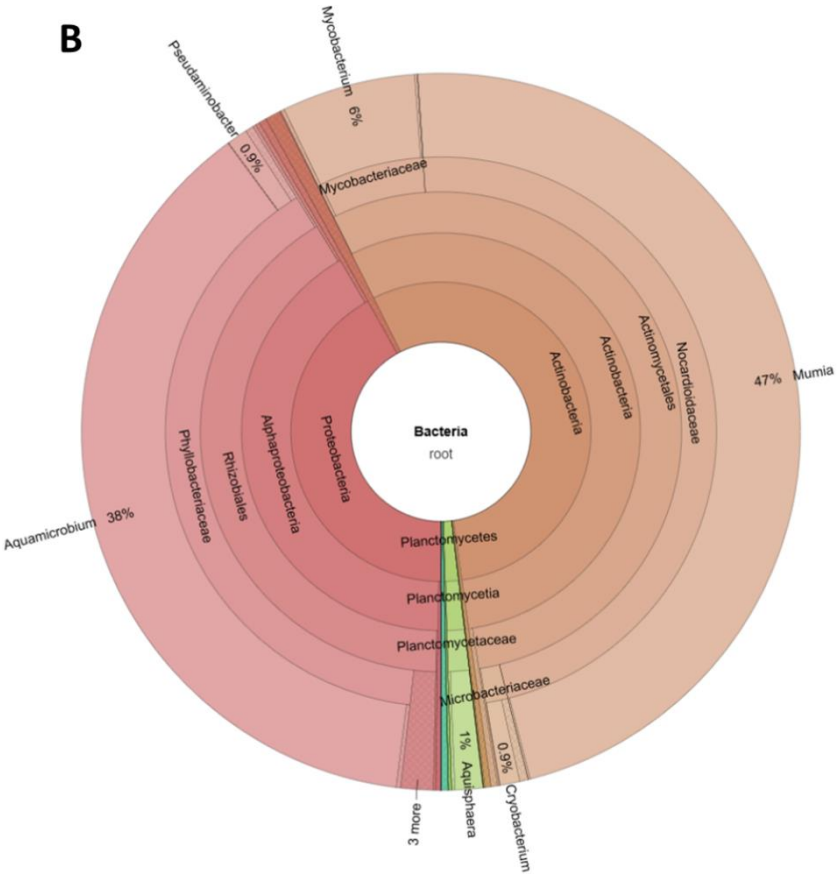

Fig. 6 Krona graphs showing the population structure of samples I-PBC (A: algal-bacterial inoculum) and F-PBC (B, end of the experimental period)

The genus *Aquamicrobium* belonging to the class *Alphaproteobacteria* showed an abundance of 38 %. Different members of the genus *Aquamicrobium* have been isolated from pollutant-loaded environments such as wastewater treatment plants, activated sewage sludge and biofilters (Jin et al. 2013). Moreover, *Aquamicrobium sp*. was recently identified as an AOB resistant to high concentrations of N-NH_4^+ (Yang et al. 2015). Similarly, Huang et al. demonstrated the capacity of *Aquamicrobium sp*. to oxidize ammonia, and classified this genus as a cold- and salt-tolerant AOB (Huang et al. 2017). Therefore, the presence of *Aquamicrobium* in the PBC cultivation broth, an AOB extremely tolerant to high temperatures and NH_4^+ concentrations, supports the hypothesis of a partial nitrification which resulted in the accumulation of nitrite over nitrate.

4. Conclusions

This study confirmed the feasibility of biologically abating TMA from waste gas streams in bacterial and algal-bacterial bubble column reactors. The bacterial reactor achieved REs of 78 % and ECs of 12 g TMA m^{-3} h^{-1} at inlet TMA concentrations of ~ 500 mg m^{-3} and EBRT of 2 min. Conversely, the algal-bacterial photobioreactor provided enhancements in TMA removal by almost 20 % and reached ECs of 16 g TMA m^{-3} h^{-1} under similar conditions. The maintenance of high TMA-REs at EBRTs of 1.5 and 1 min (98 % and 94 %, respectively) confirmed the outstanding performance of the algal-bacterial photobioreactor. The higher pH recorded in the PBC due to photosynthetic activity together with the lower nitrification rates could have mediated this enhanced performance. Moreover, algal activity in the PBC resulted in a net CO_2 consumption in the gas stream and a 30 % decrease in the TN concentration of the liquid effluent as a result of a superior nitrogen assimilation. These promising results highlight the potential of implementation of this innovative process for TMA abatement from air emissions. Likewise, this study supports the relevance of future research in order to adapt the process to the specific needs of the industrial emissions.

Acknowledgements

This work was supported by the regional government of Castilla y León and the EU-FEDER programme (UIC 71 and CLU 2017-09).

References

Aguirre A, Bernal P, Maureira D, et al (2018) Biofiltration of trimethylamine in biotrickling filter inoculated with Aminobacter aminovorans. Electron J Biotechnol 33:63–67. doi: 10.1016/j.ejbt.2018.04.004

American Water Works Association, 2012.

Standard Methods for the Examination of Water and Wastewater. American Water Works Association/American Public

Awolusi OO, Nasr M, Kumari S, Bux F (2016) Artificial Intelligence for the Evaluation of Operational Parameters Influencing Nitrification and Nitrifiers in an Activated Sludge Process. Microb Ecol 72:49–63. doi: 10.1007/s00248-016-0739-3

Borde X, Guieysse B, Delgado O, et al (2003) Synergistic relationships in algal-bacterial microcosms for the treatment of aromatic pollutants. Bioresour Technol 86:293–300. doi: 10.1016/S0960-8524(02)00074-3

Chang CT, Chen BY, Shiu IS, Jeng FT (2004) Biofiltration of trimethylamine-containing waste gas by entrapped mixed microbial cells. Chemosphere 55:751–756. doi: 10.1016/j.chemosphere.2003.11.037

Chang J-S, Show P-L, Ling T-C, et al (2017) Photobioreactors. Curr Dev Biotechnol Bioeng. doi: 10.1016/B978-0-444-63663-8.00011-2

Cole JR, Wang Q, Cardenas E, et al (2009) The Ribosomal Database Project: Improved alignments and new tools for rRNA analysis. Nucleic Acids Res. doi: 10.1093/nar/gkn879

Ding Y, Wu W, Han Z, Chen Y (2008) Correlation of reactor performance and bacterial community composition during the removal of trimethylamine in three-stage biofilters. Biochem Eng J 38:248–258. doi: 10.1016/j.bej.2007.07.011

Edgar RC (2010) Search and clustering orders of magnitude faster than BLAST. Bioinformatics. doi: 10.1093/bioinformatics/btq461

Estrada JM, Kraakman NJRB, Muñoz R, Lebrero R (2011) A Comparative Analysis of Odour Treatment Technologies in Wastewater Treatment Plants. Environ Sci Technol 45:1100–1106. doi: 10.1021/es103478j

Franco-Morgado M, Alcántara C, Noyola A, et al (2017) A study of photosynthetic biogas upgrading based on a high rate algal pond under alkaline conditions: Influence of the illumination regime. Sci Total Environ 592:419–425. doi: 10.1016/j.scitotenv.2017.03.077

Ho KL, Chung YC, Lin YH, Tseng CP (2008) Biofiltration of trimethylamine, dimethylamine,

and methylamine by immobilized Paracoccus sp. CP2 and Arthrobacter sp. CP1. Chemosphere 72:250–256. doi: 10.1016/j.chemosphere.2008.01.044

Hu J, Li DP, Liu Q, et al (2009) Effect of organic carbon on nitrification efficiency and community composition of nitrifying biofilms. J Environ Sci 21:387–394. doi: Doi 10.1016/S1001-0742(08)62281-0

Huang X, Bai J, Li K ran, et al (2017) Characteristics of two novel cold- and salt-tolerant ammonia-oxidizing bacteria from Liaohe Estuarine Wetland. Mar Pollut Bull 114:192–200. doi: 10.1016/j.marpolbul.2016.08.077

Huang Z, Gedalanga PB, Olson BH (2010) Distribution of <I>Nitrobacter</I> and <I>Nitrospira</I> Communities in an Aerobic Activated Sludge Bioreactor and their Contributions to Nitrite Oxidation. Proc Water Environ Fed 2010:2390–2403. doi: 10.2175/193864710798159101

Jin HM, Kim JM, Jeon CO (2013) Aquamicrobium aestuarii sp. nov., a marine bacterium isolated from a tidal flat. Int J Syst Evol Microbiol 63:4012–4017. doi: 10.1099/ijs.0.048561-0

Kang D, Zhao Q, Wu Y, et al (2017) Removal of nutrients and pharmaceuticals and personal care products from wastewater using periphyton photobioreactors. Bioresour Technol. doi: 10.1016/j.biortech.2017.06.153

Kim SG, Bae HS, Oh HM, Lee ST (2003) Isolation and characterization of novel halotolerant and/or halophilic denitrifying bacteria with versatile metabolic pathways for the degradation of trimethylamine. FEMS Microbiol Lett 225:263–269. doi: 10.1016/S0378-1097(03)00530-5

Klindworth A, Pruesse E, Schweer T, et al (2013) Evaluation of general 16S ribosomal RNA gene PCR primers for classical and next-generation sequencing-based diversity studies. Nucleic Acids Res. doi: 10.1093/nar/gks808

Lebrero R, Volckaert D, Pérez R, et al (2013) A membrane bioreactor for the simultaneous treatment of acetone, toluene, limonene and hexane at trace level concentrations. Water Res. doi: 10.1016/j.watres.2013.01.041

Lee LH, Zainal N, Azman AS, et al (2014) Mumia flava gen. nov., sp. nov., an actinobacterium of the family Nocardioidaceae. Int J Syst Evol Microbiol 64:1461–1467. doi: 10.1099/ijs.0.058701-0

Liffourrena AS, Lucchesi GI (2014) Degradation of trimethylamine by immobilized cells of Pseudomonas putida A (ATCC 12633). Int Biodeterior Biodegrad 90:88–92. doi: 10.1016/j.ibiod.2014.02.008

MacDonald G (2003) Biogeography: Introduction to Space, Time, and Life. Prof Geogr. doi: 10.1111/0033-0124.5502018

Magoč T, Salzberg SL (2011) FLASH: Fast length adjustment of short reads to improve genome assemblies. Bioinformatics. doi: 10.1093/bioinformatics/btr507

Markou G, Vandamme D, Muylaert K (2014) Microalgal and cyanobacterial cultivation: The supply of nutrients. Water Res 65:186–202. doi: 10.1016/j.watres.2014.07.025

Merchuk JC, Garcia-Camacho F, Molina-Grima E (2007) Photobioreactor design and fluid dynamics. Chem Biochem Eng Q 21:345–355.

Muñoz R, Guieysse B (2006) Algal–bacterial processes for the treatment of hazardous contaminants: A review. Water Res 40:2799–2815. doi: 10.1016/j.watres.2006.06.011

Muñoz R, Souza TSO, Glittmann L, et al (2013) Biological anoxic treatment of O2-free VOC emissions from the petrochemical industry: A proof of concept study. J Hazard Mater 260:442–450. doi: 10.1016/j.jhazmat.2013.05.051

Oksanen J, Blanchet FG, Kindt R, et al (2015) vegan: Community Ecology Package. R package version 2.0-10. 2013. R Packag ver 24–3. doi: 10.1007/s10265-013-0586-y

Ondov BD, Bergman NH, Phillippy AM (2011) Interactive metagenomic visualization in a Web browser. BMC Bioinformatics. doi: 10.1186/1471-2105-12-385

Oyarzun P, Alarcón L, Calabriano G, et al (2019) Trickling filter technology for biotreatment of nitrogenous compounds emitted in exhaust gases from fishmeal plants. J Environ Manage 232:165–170. doi: 10.1016/j.jenvman.2018.11.008

Perillo PM, Rodríguez DF (2016) Low temperature trimethylamine flexible gas sensor based on TiO2 membrane nanotubes. J Alloys Compd 657:765–769. doi: 10.1016/j.jallcom.2015.10.167

Schmieder R, Edwards R (2011) Quality control and preprocessing of metagenomic datasets. Bioinformatics. doi: 10.1093/bioinformatics/btr026

Vo HNP, Bui XT, Nguyen TT, et al (2018) Effects of nutrient ratios and carbon dioxide bio-sequestration on biomass growth of Chlorella sp. in bubble column photobioreactor. J Environ Manage 219:1–8. doi: 10.1016/j.jenvman.2018.04.109

Wan S, Li G, Zu L, An T (2011) Bioresource Technology Purification of waste gas containing high concentration trimethylamine in biotrickling filter inoculated with B350 mixed microorganisms. Bioresour Technol 102:6757–6760. doi: 10.1016/j.biortech.2011.03.059

Wang Q, Garrity GM, Tiedje JM, Cole JR (2007) Naïve Bayesian classifier for rapid assignment of rRNA sequences into the new bacterial taxonomy. Appl Environ Microbiol.

doi: 10.1128/AEM.00062-07

Wei Z, Huang Q, Ye Q, et al (2015) Thermophilic biotrickling filtration of gas-phase trimethylamine. Atmos Pollut Res 6:428–433. doi: 10.5094/APR.2015.047

Xue N, Wang Q, Wang J, et al (2013) Odorous composting gas abatement and microbial community diversity in a biotrickling filter. Int Biodeterior Biodegrad 82:73–80. doi: 10.1016/j.ibiod.2013.03.003

Yang X, Liu L, Wu B, et al (2015) [Screening and ammoxidation characteristics of an ammonium oxidizing bacteria group]. Wei Sheng Wu Xue Bao 55:1608—1618.

Zhang C, Yuan X, Luo Y, Yu G (2018) Prediction of species concentration distribution using a rigorous turbulent mass diffusivity model for bubble column reactor simulation part I: Application to chemisorption process of CO 2 into NaOH solution. Chem Eng Sci 184:161–171. doi: 10.1016/j.ces.2018.03.031

Zhang T, Shao MF, Ye L (2012) 454 Pyrosequencing reveals bacterial diversity of activated sludge from 14 sewage treatment plants. ISME J 6:1137–1147. doi: 10.1038/ismej.2011.188